Int j simul model 24 (2025) 1, 41-52
Original scientific paper

SIMULATION OF ELECTRIC MULTIPLE UNITS WITH VIRTUAL CONTROL UNITS

Liang, B. C.[*,#] & Zhao, H. W.[**]
[*] Postgraduate Department, China Academy of Railway Sciences, Beijing 100081, China
[**] Locomotive & Car Research Institute, China Academy of Railway Sciences Corporation Ltd., Beijing 100081, China
E-Mail: 15201341631@163.com ([#] Corresponding author)

Abstract
To effectively improve the overdependence of traditional simulation platforms on physical equipment, this study proposes a simulation platform based on a virtual central control unit (CCU) and a traction control unit (TCU). First, a traction system model was established, analysed and implemented. Second, the functions of CCU and TCU were designed, the data communication between the virtual model and physical equipment were implemented. Lastly, the operating effects of the simulation platform under operating scenarios were explored through simulation experiments and compared with the data of real vehicles. Results show that the simulation platform based on the virtual CCU is consistent with the existing simulation platforms in operating effect, meeting the needs of interconnectivity experiments. The simulation model requires 377 s to accelerate from 0 to 350 km/h, and the speed loss in neutral-zone passing is 22.1 km/h at most at the speed of 350 km/h, which is approximate to the real data. The obtained conclusions are of realistic significance for establishing an interconnected simulation test platform specific to electric multiple units of different models.
(Received in October 2024, accepted in January 2025. This paper was with the authors 1 month for 1 revision.)

Key Words: Traction Drive System Simulation, Central Control Unit Simulation, Simulation Platform Construction, Neutral-Zone Passing

1. INTRODUCTION

High-speed rail, as an important mode of transportation, calls for intelligence development in a new era. All countries around the world are carrying out new research on the intelligence of transportation facilities. In the technical system of intelligent high-speed railways, key system simulation, which is a vital part of intelligent equipment technology, is listed as one of the key research contents. Simulation technology has been widely applied in various fields, such as component optimization [1], train scheduling [2], and system testing [3]. With the continuous development of such technologies as digital twins and artificial intelligence [4], the demand of the simulation of electric multiple units (EMUs) has gradually developed from a single system to multiple systems, and the concept of EMU simulation platform has gradually emerged. With the completion of the intelligent Beijing–Zhangjiakou Railway, intelligent high-speed railways have ushered in a new stage of development, and establishing a simulation platform that can reflect the running state of EMUs is of evident realistic significance [5].

Given different modelling methods, models will have diverse forms and can be transformed into various simulation models running on the same simulation platform by adopting appropriate programming language. Current simulation platforms of EMUs are mostly based on hardware-in-the-loop (HIL) simulation [6]. In the construction scheme, the central control unit (CCU) is the core equipment. CCU can handle the message sent to it in accordance with the running logic and then automatically send messages itself, presenting the results on a human–machine interface (HMI). During the whole simulation period, the internal logic of CCU is invisible and can hardly be changed.

This construction scheme is subject to three defects. First, the models of controlled objects such as traction control unit (TCU) and braking control unit are not established. Speed information for CCU is obtained by combining the external instruction and the built-in simple model operation, and data interaction between TCU and CCU is not realized in the network, which differs from the real running status [7]. Second, because EMUs are fabricated by different manufacturers, the CCU hardware circuits used vary, and the content of messages sent does not conform to the same protocol. Thus, the simulation platform needs to be separately designed for the EMUs of different models. Additional time should be spent in modifying CCU to realize the interconnectivity of EMUs in different models, which increases the difficulty in the double heading test. Third, CCU physical equipment is adopted for such simulation platforms, so all functions of the whole simulation platform will fail in case of any fault due to circuit aging of the equipment, thereby increasing the maintenance cost.

The operation of EMUs requires not only the implementation of hardware and software but also the interface between systems [8]. Therefore, the communication network applied to EMUs should be considered when establishing the simulation platform. On the existing EMUs, the network based on multifunction vehicle bus (MVB) and wire train bus (WTB) is generally used. On new-type EMUs, Ethernet is now widely adopted, and wireless networks may also be used on future EMUs. The message sending method cannot be freely changed if CCU has a physical form, and the message content adopted by each communication mode may not be necessarily the same. Hence, CCU and the corresponding simulation platform should be remanufactured once a new network communication technology is used, which greatly increases the platform construction cost.

To reduce the construction cost of the platform and the difficulty of the interconnectivity test, this study designed simulation modelling of virtual CCU, which provided an experimental basis for the test of different vehicle models. The general interconnectivity test only requires testing CCU. Here, TCU was also subject to simulation modelling, and different operating conditions were established to elevate the fidelity of the simulation platform.

2. STATE OF THE ART

In the field of EMUs, the simulation study is generally oriented to specific physical equipment, such as pantograph, wheel, or running line [9], lacking a system-level overall simulation or a network communication simulation of control unit functions. System research generally focuses on the evaluation of energy consumption [10] and control strategies [11]. Davidyan et al. [12] developed a digital twin model for truck braking systems and proved the broad application prospects of digital simulation technology in the field of EMUs.

Traction system modelling plays a critical role in EMUs simulation. Ftorek et al. [13] established a motor driving model and a speed calculation model based on energy optimal control using MATLAB, focusing on the verification of algorithm strategy. Consequently, the established model failed to restore the real operation situation. Sovicka et al. [14] performed a train simulation based on a mathematical model with MATLAB and realized a train speed controller and a simple graphical user interface but failed to attain CCU and TCU with complete functions. Bilbao-Moreno et al. [15] used MATLAB to construct a traction drive system including the influence of air resistance and tractive effort, with the research emphasis laid on testing the automatic driving algorithm, so the communication between CCU and TCU was not realized. Butdee [16] established a driving simulation system by C language programming and obtained a virtual operation interface but neither realized communication with external hardware devices nor tested the simulation data. Johansson et al. [17] created a macro-operation simulation model by using RailSys tool, but this model was mainly aimed at

macro-operation scenarios; hence, the working conditions of micro-operation during operation were not simulated.

All the above studies have been carried out through pure software-based simulation. Except for the platform carrying the simulation model, other hardware devices are not involved. In creating an HIL simulation platform, data interaction with hardware equipment should be incorporated, making it necessary to establish the functions of TCU.

In the modelling research involving TCU, Li et al. [18] used the hardware architecture of a real CCU and a virtual TCU to realize a distributed simulation platform of an electric traction system. However, the simulation platform was designed for a 600 km/h maglev train and is not suitable for standard EMUs. Herrero et al. [19] used a real TCU to establish an HIL simulation platform, which realized complete simulation of the traction system but not the function of CCU.

In the test of the abovementioned studies, only the conventional working conditions have been generally verified, and the scenario of neutral-zone passing has not been considered. Neutral-zone passing is a special scenario generated to cooperate with power supply segmentation during running. In an actual running process, the failure probability is high in neutral-zone passing scenarios. The current research regarding neutral-zone passing scenarios mainly concentrates on new neutral-zone passing control methods [20], while the speed loss and signal controlling of EMUs in the neutral zone have been rarely involved.

Few studies exist on CCU modelling. Gao et al. [21] established a new CCU architecture with enhanced safety, which can meet the requirements of safety integrity level four. However, this architecture used a physical CCU, which is without work-scenarios analysing. Li [22] built a simulated CCU based on CRH380B EMU, which can realize all the functions of a real CCU. However, the CCU was only subject to a braking test, and a WTB/MVB network, instead of Ethernet, was adopted as the communication mechanism.

The existing studies mainly focus on simulation modelling of traction drive systems and CCU. On the one hand, in the simulation process of traction drive systems, only the conventional conditions such as traction and braking under a single vehicle model are tested, and the functionality of scenarios remain to be improved. On the other hand, the function realization of control units such as CCU and TCU has been rarely studied. In most simulation studies, only the drive process has been investigated, without transferring simulation data as one part of the simulation platform to other devices. As a result, these simulation system studies stay on pure software implementation, failing to form a hardware-in-the-loop simulation platform with general hardware devices. In this study, virtual CCU and TCU were set up based on EMUs of two different models – CR400AF and CR400BF – produced by different manufacturers, aiming to realize real-time communication with physical equipment and a simulation model under the Ethernet protocol. On this basis, different running scenarios of EMUs were established, the performance of the simulation system under four scenarios – traction, constant speed, braking, and neutral-zone passing – was analysed and compared with that of a real drive system, and the neutral-zone passing scenarios of different vehicle models were tested. Moreover, the speed loss was assessed, providing technical support for the subsequent research.

The remainder of this study is organized as follows: In the “Methodology” section, simulation models are created for the traction drive system and the control unit. In the “Results analysis and discussion” section, various operating conditions are defined, the simulation data is compared with the field test data and the effectiveness of the simulation model is demonstrated. In the final section, the entire study is summarised and relevant conclusions are drawn.

3. METHODOLOGY

3.1 Traction simulation

During the running process of EMUs, three forces of tractive effort, air resistance, and braking force, exert influences regardless of line conditions, among which tractive effort and braking force are controllable. EMUs run under three conditions: traction, braking, and coasting. Tractive effort and air resistance function under traction condition, braking force and air resistance function under braking condition, and only air resistance functions under coasting condition.

TCU generally controls the output tractive effort by regulating the motor torque, and the relationship between the torque and tractive effort is calculated as follows:

$$T_{ref} = \frac{Fr}{Na\eta} \tag{1}$$

where T_{ref} is the output torque; r is the radius of solid wheel, taken as 0.46 m; N is the number of transmission shafts, taken as 16; a is the gear ratio, taken as 2.517; η stands for motor efficiency, taken as 94 %.

The tractive effort and regenerative braking force provided by the simulation model are calculated in accordance with the characteristic curve in the technical conditions, and the specific calculation formula for tractive effort as shown in Eq. (2).

$$F = \begin{cases} 276 - 0.375v, & 0 < v \le 160 \\ \dfrac{34560}{v}, & 160 < v \le 350 \end{cases} \tag{2}$$

The specific calculation formula for regenerative braking force is shown as follows.

$$F = \begin{cases} 0, & 0 < v \le 2 \\ 34(v-2), & 2 < v \le 10 \\ 272 - 0.2267(v-10), & 10 < v \le 160 \\ \dfrac{38016}{v}, & 160 < v \le 350 \end{cases} \tag{3}$$

where F is the value of tractive effort/braking force, and v is the running speed of EMUs.

The resistance calculated by factors including air resistance and component friction during train operation is calculated as shown in Eq. (4).

$$\begin{aligned} F_{\mathrm{AF}} &= 1.6 + 0.0111v + 0.000473v^2 \\ F_{\mathrm{BF}} &= 2.0 + 0.062v + 0.000535v^2 \end{aligned} \tag{4}$$

where F_{AF} is the running resistance of CR400AF EMUs, F_{BF} is the running resistance of CR400BF EMUs, and v is the running speed of EMUs.

Combining tractive effort/braking force and resistance, the resultant force of the train can be acquired to calculate the acceleration, which is affected by the slope of the line. The slope is generally expressed by permillage, defined as the height difference between the endpoint and starting point when the train runs by 1000 m. According to the conversion, if the EMU is considered as a single-mass-point model, the acceleration change induced by the slope is only related to the slope and the gravitational acceleration, meaning that the existence of the slope can be judged by the acceleration change.

The speed can be acquired by time integration with acceleration, followed by integration once again to acquire the mileage. In this simulation, the mass of CR400AF was set to 474 t and that of CR400BF to 490 t. Acceleration, speed, and milage are the important outputs of the traction drive system and significant information transmitted to CCU, as shown in Fig. 1.

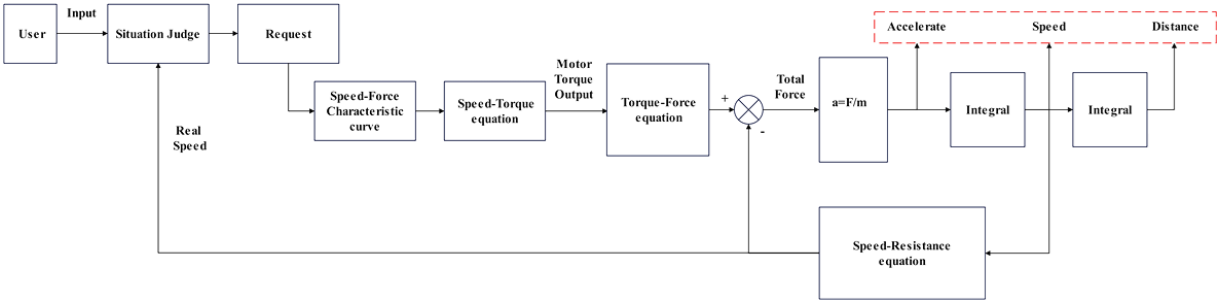

Figure 1: Speed and mileage calculation module.

The resultant force on EMUs is only related to the speed on the premise of unchanged conditions of the line by using Eqs. (2) to (4). Against this backdrop, a BP neural network model can be used to depict the nonlinear relationship between speed and acceleration for reducing test cost and improving the functional capabilities of the simulation platform.

3.2 Platform framework

In the virtual digital train simulation platform set up in this study, a software platform was taken as the carrier to construct CCU, data receiving and transmitting module, and key subsystems (i.e., each subsystem simulation model contains subsystem control units and their controlled objects).

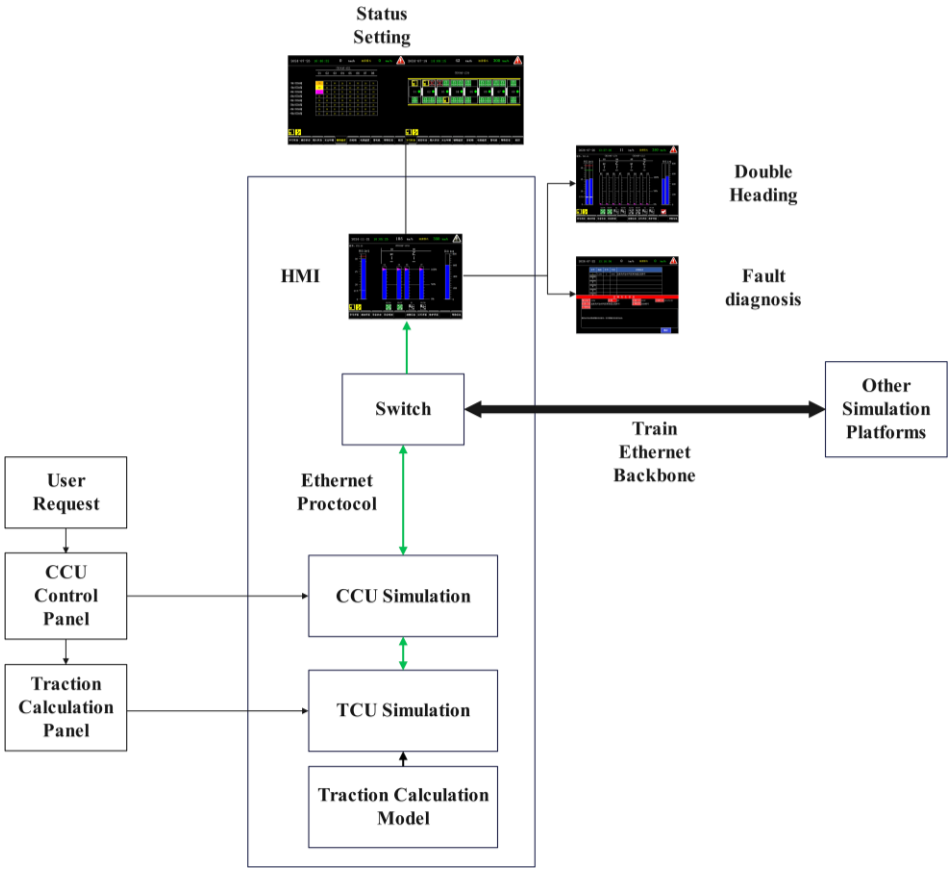

Figure 2: Design scheme of the virtual train simulation platform.

Fig. 2 offers a visualisation of the overall architecture scheme of the simulation platform. According to the protocol, CCU needs to transmit and receive considerable data; hence, numerous front panels will be needed in the CCU simulation, including process data panel, subsystem data panel, and driver control consoles.

Through realizing the internal logic of CCU and discovering the linkage characteristics of data bits, the operation complexity can be reduced, and the running effect of the virtual CCU can be closer to reality. Owing to the absence of relevant documents about the linkage of data bits in CCU, the control logic of the virtual CCU was finally realized with reference to the test performance of the physical CCU.

Figure 3: Virtual digital train simulation platform.

Fig. 3 delineates the hardware of simulation platform. After testing, the simulation platform can be reconnected with other simulation platforms and can realize double heading and meet the requirements of interconnectivity testing. The virtual CCU has the same function as the real CCU, which can affect the results presented by HMI by changing the data bits on the front panel of the virtual CCU, including routine driver operations such as lifting the pantograph, closing the main circuit, and adjusting the traction level, as well as setting the train state information such as axle temperature, door state, and loop state.

4. RESULTS ANALYSIS AND DISCUSSION

4.1 Traction process

After the normal function of the virtual CCU simulation platform is ensured, the established traction drive model will be subject to simulation and verification, testing whether it meets the real vehicle design standard and comparing it with the actual test data.

The target speed was set to 350 km/h; the net voltage was normal by default; the traction motor had no fault, with the level set to Level 7, and it was free from the influence of the slope and tunnel; the EMUs model was CR400AF. The simulation results under the traction condition with the influence of air resistance are listed in Table I.

Table I: Running stages of traction process.

Running speed (km/h)	**Running time** (s)	**Residual acceleration** (m/s^2)	**Running distance** (km)
0	0	0.57	0
50	24.8	0.54	0.18
100	51.4	0.49	0.74
150	80.7	0.45	1.76
200	116.8	0.31	3.53
250	169.0	0.22	6.81
300	245.6	0.15	12.7
350	376.6	0.05	24.6

The whole acceleration process took 377 s, and the acceleration distance was 24.6 km, the average acceleration from 0 km/h to 200 km/h was 0.48 m/s^2, which was no less than 0.4 m/s^2, and the residual acceleration after reaching 350 km/h was 0.05 m/s^2, which was in line with the running characteristics of the real vehicle. The comparison between real vehicle test data and simulation data is shown in Fig. 4.

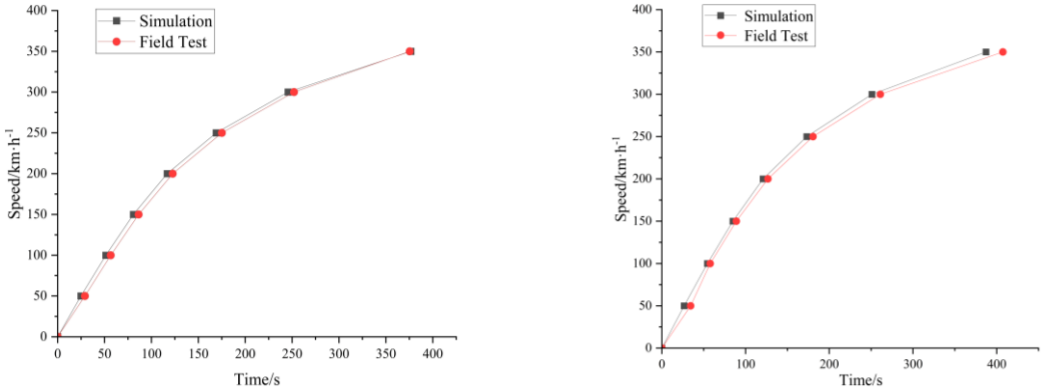

a) CR400AF b) CR400BF

Figure 4: Comparison between simulated traction process and field vehicle traction test.

Fig. 4 illustrates that the field vehicle test results were close to the simulation results, which verify the effectiveness of the simulation model. Neural network training was performed using the data of this simulation model. Specifically, for simulating the scenario with unknown traction system parameters, only the model-output speed was acquired. The acceleration was obtained by means of difference. The BP neural network was trained with speed as the input and acceleration as the output, and verification was implemented using the real speed and acceleration data of this model. The results are exhibited in Fig. 5.

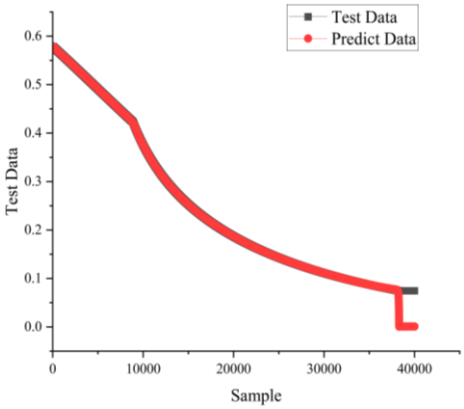

Figure 5: Acceleration predicted via neural networks during traction process.

Fig. 5 presents a good consistence between the predicted acceleration and the training goal, although an error appeared in the data of the last section. The error was due to the residual acceleration after the target set speed in the actual running traction system was reached. The residual acceleration at this time could not be calculated when the speed difference was used to calculate the acceleration. Hence, the predicted acceleration was 0 in this case. Nevertheless, the error, which was within an acceptable range, did not affect the overall result. The BP Neural Network proposed in this study has a classification accuracy rate of 95.69 % and root mean square error value of 0.02. Thus, the efficacy of the proposed model is emphasized, displaying high accuracy in the real-time condition monitoring of EMUs acceleration.

4.2 Constant-speed process

In the running process of the train, additional resistance will be generated while going up the slope, and additional acceleration will be generated while going down the slope. The slope of the line was adjusted under different initial speeds. A positive slope indicates going up the slope and a negative one means going down the slope. The simulation results are displayed in Table II.

Table II: Constant-speed capacity test under different initial speeds and slopes.

Initial speed (km/h)	**Slope**	**AF Steady speed** (km/h)	**BF Steady speed** (km/h)
350	+15 ‰	327	326.2
	+5 ‰	346.7	346.5
	−5 ‰	350	350
	−15 ‰	352.1	351.6
250	+15 ‰	246.5	246.5
	+5 ‰	248.1	248.2
	−5 ‰	250	250
	−15 ‰	252.7	252.6
160	+15 ‰	157.6	157.7
	+5 ‰	158.5	158.6
	−5 ‰	162.1	162.1
	−15 ‰	162.7	162.7

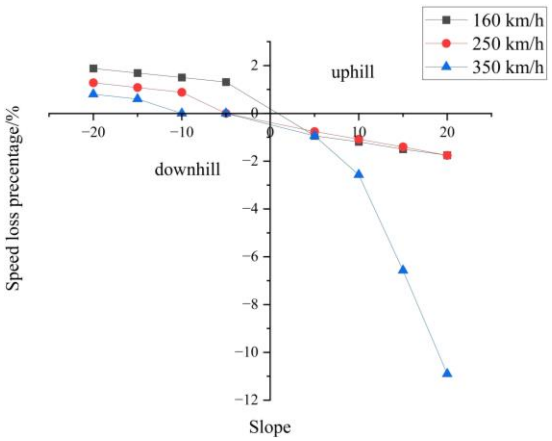

Figure 6: Speed loss when occurring slope with different initial speed.

Fig. 6 displays the percentage of speed loss of different initial speeds of CR400AF when occurring slope. Higher the speed, lower the uphill slope that could be borne, and higher the downhill slope that could be borne. The reason was that higher the speed, lower the tractive effort output and the greater the air resistance, making it easier to lose speed when going up the slope and maintain speed when going down the slope.

4.3 Braking process

The regenerative braking ability of CR400AF EMUs was tested by reducing the expected speed from 350 km/h to 0 km/h. For reproducing the real characteristic of regenerative braking, the deceleration effect induced by air resistance and slope was no longer calculated in the simulation environment. The operation results are presented in Table III.

Table III: Running stages of braking process (air resistance-free).

Running speed (km/h)	**Running time** (s)	**Residual deceleration** (m/s^2)	**Staged deceleration** (m/s^2)
350	0	0.23	0
240	112.3	0.33	0.27
160	167.7	0.50	0.40
20	240.5	0.57	0.53
5	248.7	0.29	0.51

The regenerative braking force gradually increased with the decrease in EMU speed, decreased rapidly until the speed decreased to below 10 km/h, and completely returned to zero when the speed decreased to below 2 km/h, so the final speed in the simulation results slowly approached 2 km/h. The running time for CR400AF EMU to decelerate from 350 km/h to 5 km/h by regenerative braking was 248.7 s, and the braking distance was 14.3 km. The simulation results were compared with the deceleration test results of service braking in the real vehicle running test, as shown in Fig. 7.

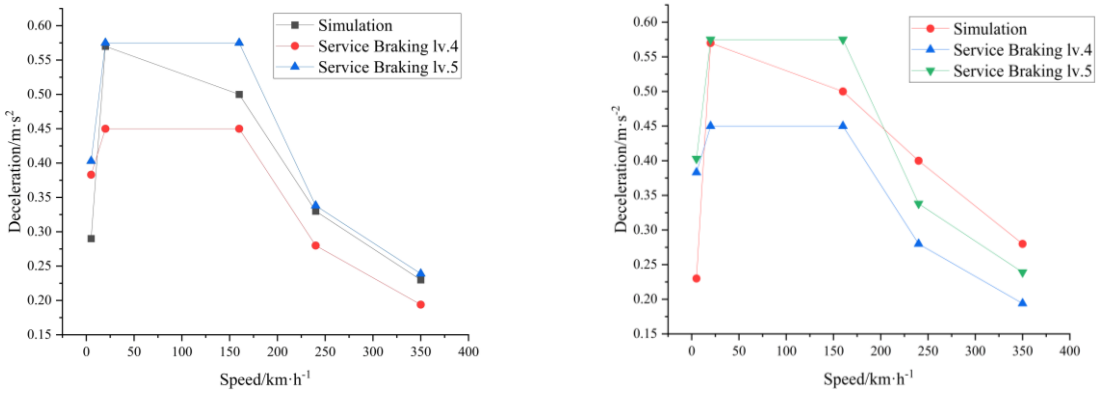

a) CR400AF b) CR400BF

Figure 7: Comparison between simulated and real vehicle braking processes.

In Fig. 7, the deceleration characteristics of regenerative braking proposed by simulation were between four-stage service braking and five-stage service braking, which was in line with expectations and verified the effectiveness of the simulation model.

4.4 Neutral-zone passing

Neutral-zone passing is a special state of EMU in operation, which can be subdivided into four situations: automatic train protection (ATP), magnetic induction system (MIS), manual, and over distance neutral-zone passing. ATP and MIS neutral-zone passing are formal scenarios, and the related distance and time are documented; thus, they can be analysed in detail. Manual neutral-zone passing is a scenario largely influenced by the driver's experience, and the simulation scenario will be quite different from the real scenario. Over distance neutral-zone passing is a fault scenario, which is caused by the abnormal missing of out-of-neutral-zone signal. Under the neutral-zone passing scenario of a single EMU at an initial speed of 200 km/h for example, the process of neutral-zone passing is displayed in Fig. 8.

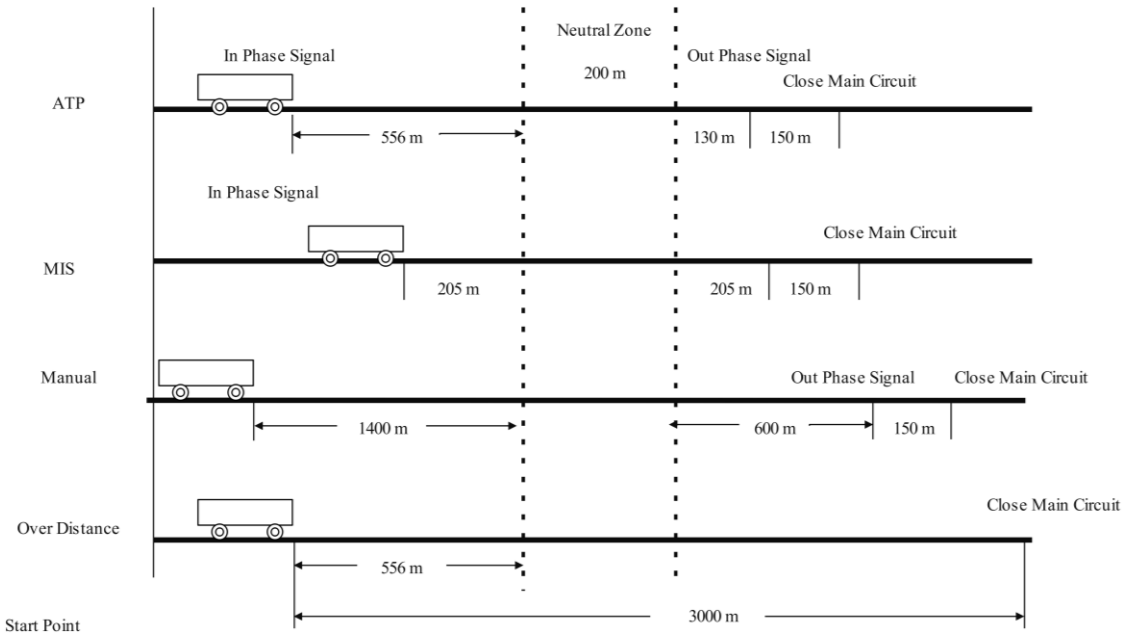

Figure 8: Neutral-zone passing process nodes.

Different initial speeds, vehicle models, and neutral-zone passing modes were set for the neutral-zone passing test under the same conditions of the line, and the results are listed in Table IV. To maintain medium voltage of EMU, the minimum speed should be no less than 55 km/h.

Table IV: Neutral-zone passing simulation results.

			CR400AF			CR400BF		
Initial speed (km/h)	**Signal type**	**Running distance** (m)	**Duration** (s)	**Minimum speed** (km/h)	**Speed loss** (km/h)	**Duration** (s)	**Minimum speed** (km/h)	**Speed loss** (km/h)
80	ATP	702	34.8	66.3	13.7	35.3	65.6	14.4
	MIS	760	37.9	65.0	15.0	38.1	64.1	15.9
	Manual	2350	141.5	52.9	27.1	144.0	50.7	29.3
	Over distance	3000	186.3	51.6	28.4	191.4	48.5	31.5
120	ATP	813	25.2	112.6	7.4	25.4	111.4	8.6
	MIS	760	23.6	113.1	6.9	23.7	112.0	8.0
	Manual	2350	78.1	96.0	24.0	79.6	92.3	27.7
	Over distance	3000	103.7	87.4	32.6	106.5	82.3	37.7
160	ATP	924	21.3	154.3	5.7	21.3	152.7	7.3
	MIS	760	17.4	155.3	4.7	17.7	154.1	5.9
	Manual	2350	55.7	144.9	15.1	56.6	140.9	19.1
	Over distance	3000	72.2	139.8	20.2	73.2	135.1	24.9
200	ATP	1036	19.0	194.3	5.7	19.0	192.7	7.3
	MIS	760	13.9	195.8	4.2	13.9	194.7	5.3
	Manual	2350	43.8	186.9	13.1	44.2	183.3	16.7
	Over distance	3000	56.4	183.3	16.7	57.1	178.5	21.5
250	ATP	1174	17.2	243.9	6.1	17.2	242.0	8.0
	Manual	2350	34.7	237.7	12.3	35.0	233.9	16.1
	Over distance	3000	44.6	234.3	15.7	45.1	229.5	20.5
300	ATP	1313	16.0	293.0	7.0	16.0	290.8	9.2
	Manual	2350	28.8	287.5	12.5	29.0	283.5	16.5
	Over distance	3000	37.0	284.0	16.0	37.4	279.0	21.0
350	ATP	1452	15.3	341.9	8.1	15.7	339.3	10.7
	Manual	2350	24.7	336.8	13.2	25.2	332.6	17.4
	Over distance	3000	31.7	330.0	20.0	32.1	327.9	22.1

Table IV provides the following conclusions: When ATP and MIS worked normally and the speed reached 80 km/h or above, CR400AF/BF single EMU could maintain the medium voltage and pass through the neutral zone by 200 m. When the neutral zone was passed, the speed loss of AF EMUs was generally lower than that of BF EMUs.

5. CONCLUSION

To meet the interconnectivity needs of EMUs of different models, this study established a simulation platform based on virtual CCU and TCU and tested it under four working conditions: traction, constant speed, braking, and neutral-zone passing. The following conclusions were drawn:

The functions of the virtual CCU, such as reconnecting with the real CCU, state setting and message receiving, were verified to meet the interconnectivity test needs. Through building CCU and TCU by virtual software, the system development cost was reduced, the expansibility of the platform was enhanced, and the problems of the former CCU simulation system (e.g., reliance on physical equipment, difficulty in fault positioning, and unclear logic) were solved. Through the scenario test we presented, the simulation model exhibits good consistency with the field experimental data and can reflect the actual running status well.

In this study, virtual CCU and TCU were applied to the simulation platform, which could realize a consistent running effect with the physical equipment, thereby reducing the cost of interconnectivity test, effectively improving the fidelity of the simulation platform, and reducing the time of fault diagnosis caused by the physical CCU device. This study contributes a practical solution to intelligent railway simulation and the improvement of EMU interconnectivity test.

ACKNOWLEDGEMENT

This work was supported by the key project of China State Railway Group Co., Ltd (Grant No.: N2022J0006).

REFERENCES

[1] Calvo Hernandez, A.; Sanz Bobi, J. de D.; Gomez Fernandez, J.; Badolato Martin, A (2021). Vibration reduction on overhead contact rails: a simulation-optimization approach, *International Journal of Simulation Modelling*, Vol. 20, No. 2, 315-326, doi:10.2507/IJSIMM20-2-561

[2] Jones, W.; Gun, P. (2024). Train timetabling and destination selection in mining freight rail networks: a hybrid simulation methodology incorporating heuristics, *Journal of Simulation*, Vol. 18, No. 1, 1-14, doi:10.1080/17477778.2022.2056536

[3] Cunha, J.; Reis, V.; Teixeira, P. (2022). Development of an agent-based model for railway infrastructure project appraisal, *Transportation*, Vol. 49, No. 6, 1649-1681, doi:10.1007/s11116-021-10223-2

[4] Raiaan, M. A. K.; Mukta, M. S. H.; Fatema, K.; Fahad, N. M.; Sakib, S.; Mim, M. M. J.; Ahmad, J.; Ali, M. E.; Azam, S. (2024). A review on large language models: architectures, applications, taxonomies, open issues and challenges, *IEEE Access*, Vol. 12, 26839-26874, doi:10.1109/ACCESS.2024.3365742

[5] Wang, T. (2021). The intelligent Beijing–Zhangjiakou high-speed railway, *Engineering*, Vol. 7, No. 12, 1665-1672, doi:10.1016/j.eng.2021.10.006

[6] Mihalič, F.; Truntič, M.; Hren, A. (2022). Hardware-in-the-loop simulations: a historical overview of engineering challenges, *Electronics*, Vol. 11, No. 15, Paper 2462, 34 pages, doi:10.3390/electronics11152462

[7] IEEE (2024). *IEEE Std 2950-2024: IEEE standard for electric traction system for high-speed electric multiple units (EMUs)*, 26 pages, Piscataway, doi:10.1109/IEEESTD.2024.10616044

[8] Zhao, H.; Huang, Z.; Mei, Y. (2017). High-speed EMU TCMS design and LCC technology research, *Engineering*, Vol. 3, No. 1, 122-129, doi:10.1016/J.ENG.2017.01.004
[9] Montenegro, P. A.; Carvalho, H.; Ribeiro, D.; Calçada, R.; Tokunaga, M.; Tanabe, M.; Zhai, W. M. (2021). Assessment of train running safety on bridges: a literature review, *Engineering Structures*, Vol. 241, Paper 112425, 23 pages, doi:10.1016/J.ENGSTRUCT.2021.112425
[10] Hamedani, P.; Fazel, S. S.; Shahbazi, M. (2025). Energy consumption assessment in a DC electric railway system with regenerative braking: a case study of Isfahan metro line 1, *International Journal of Engineering*, Vol. 38, No. 3, 528-538, doi:10.5829/ije.2025.38.03c.02
[11] Ahmad, S.; Saeed, M.; Guerrero, J. M.; Muniategui-Aspiazu, I.; Nuñez, G.; Larrazabal, I.; Briz, F. (2025). Priority-based DC-link voltage control for railway traction chains with onboard energy storage, *IEEE Open Journal of Industry Applications*, Vol. 6, 1-14, doi:10.1109/OJIA.2024.3501072
[12] Davidyan, G.; Bortman, J.; Kenett, R. S. (2024). Development of an operational digital twin of a freight car braking system for fault diagnosis, *Advanced Theory and Simulations*, Vol. 7, No. 6, Paper 2301257, 11 pages, doi:10.1002/adts.202301257
[13] Ftorek, B.; Šimon, J.; Kiselev, M.; Vavrúš, V.; Vittek, J. (2022). Exploitation of energy optimal and near-optimal control for traction drives with AC motors, *Symmetry*, Vol. 14, No. 12, Paper 2613, 14 pages, doi:10.3390/sym14122613
[14] Sovicka, P.; Pacha, M.; Rafajdus, P.; Varecha, P.; Zossak, S. (2019). Improved train simulation with speed control algorithm, *Transportation Research Procedia*, Vol. 40, 1563-1570, doi:10.1016/j.trpro.2019.07.216
[15] Bilbao-Moreno, D.; Elorza, I.; Irigoyen, E. (2024). Development of a software platform for automatic train operation: integrating meso- and microscopic layers, *Results in Engineering*, Vol. 24, Paper 103129, 17 pages, doi:10.1016/j.rineng.2024.103129
[16] Butdee, S. (2019). Simulation on high speed train with driving algorithm and rules for operation image control, *Procedia Manufacturing*, Vol. 30, 575-580, doi:10.1016/j.promfg.2019.02.081
[17] Johansson, I.; Palmqvist, C.-W.; Sipilä, H.; Warg, J.; Bohlin, M. (2022). Microscopic and macroscopic simulation of early freight train departures, *Journal of Rail Transport Planning & Management*, Vol. 21, Paper 100295, 14 pages, doi:10.1016/j.jrtpm.2022.100295
[18] Li, T.; Wang, M.; Qin, Y.; Wu, X.; Li, D.; Yang, P.; Ding, R.; Yang, J. (2024). Distributed virtual simulation experimental software for high-power electric traction system of 600 km/h high-speed maglev train, *Advances in Engineering Software*, Vol. 192, Paper 103627, 18 pages, doi:10.1016/j.advengsoft.2024.103627
[19] Herrero, M. M.; Mendez, A. R.; Caballo, I. C.; Aspiazu, I. M.; Arza, J. (2024). Hardware-in-the-loop platform for virtual certification of traction systems for railway, *IEEE Access*, Vol. 12, 52182-52194, doi:10.1109/ACCESS.2024.3387347
[20] Mcineka, C. T.; Pillay, N.; Moorgas, K.; Maharaj, S. (2024) Automatic switching of electric locomotive power in railway neutral sections using image processing, *Journal of Imaging*, Vol. 10, No. 6, Paper 142, 20 pages, doi:10.3390/jimaging10060142
[21] Gao, F.; Liang, H.; Zhang, K.; Li, Y. (2022). Safety enhancement design method and control strategy for CCU of high-speed train, *Advances in Mechanical Engineering*, Vol. 14, No. 4, Paper 16878132221089806, 12 pages, doi:10.1177/16878132221089806
[22] Li, B. (2018). Design of simulated CCU used for high-speed EMU engineers training, *2018 9th International Conference on Information Technology in Medicine and Education (ITME)*, 770-774, doi:10.1109/ITME.2018.00174